Appl. Phys. B 79, 435–439 (2004)
DOI: 10.1007/s00340-004-1555-x

Applied Physics B
Lasers and Optics

W. WOHLLEBEN[1,*]
J. DEGERT[2,**]
A. MONMAYRANT[2]
B. CHATEL[2]
M. MOTZKUS[1,*]
B. GIRARD[2,✉]

Coherent transients as a highly sensitive probe for femtosecond pulse shapers

[1] MPI für Quantenoptik, 85748 Garching, Germany
[2] Laboratoire de Collisions, Agrégats, Réactivité (CNRS UMR 5589), IRSAMC, Université Paul Sabatier, 31062 Toulouse, France

Received: 19 December 2003/Revised version: 21 April 2004
Published online: 16 June 2004 •

ABSTRACT We report on the application of shaped femtosecond pulses on low-field chirped excitation of an atomic two-level system. The induced transient phenomena can be considered as a phase diagram of the excitation pulse. Their high sensitivity to the phase-modulated pulse is analyzed, by comparing numerical solutions of the time-dependent Schrödinger equation with experimental results. These coherent transients allow for high precision calibration of pulse-shaping setups where usual methods are less efficient. As an illustration, a comparison between 128-pixel and 640-pixel spatial light modulator pulse shapers is given.

PACS 32.80.Qk; 42.50.Md; 42.65.Re; 82.53.Kp

1 Introduction

Atomic transitions with few levels offer an ideally suited benchmark system to illustrate the ultimate resolution and fidelity of femtosecond pulse shaping. Due to the simplicity of the system, theory is sufficiently reliable and provides an efficient comparison with the experiment. A very basic phenomenon of matter-light interaction that is nonetheless apt for control with shaped femtosecond pulses is the chirped excitation of a two-level system [1–6]. The excited state population exhibits Coherent Transients (CT) due to interferences between the instantaneous electric field and the dipole excited at resonance [1]. This 'self induced heterodyne' effect has been exploited to characterise the value of the linear chirp [7, 8]. Any phase modulation applied in addition to the linear chirp will produce a large effect on the CT at the corresponding time interval [2, 9]. Indeed by virtue of the time to frequency correspondence for a strong chirp, the CT interference pattern represents a phase diagram of the excitation spectrum. As we will demonstrate in the following, its sensitivity exceeds the 10^{-4} level and it is, thus, an appropriate probe for steeply shaped light fields. The most common devices for both high fidelity and wide flexibility of shapes involve an optical Fourier plane where a liquid crystal spatial light modulator (SLM) [10], acousto-optic modulator [11] or deformable mirror [12] modulates the spectral phase and/or amplitude. Here the resolution is independent of the spectral bandwidth but limited by the $4-f$-line parameters and the smallest adjustment of the shaping device e.g., the SLM pixel size. Shaping without Fourier transform optics is also possible by using an actively controlled acousto-optic programmable filter [13]. In this case the resolution is mainly limited by the laser bandwidth and the length of the crystal.

Here we report on experiments that use the resonant excitation of a two-level system by a chirped pulse with an additional spectral phase to check the ultimate quality of the pixellated liquid crystal pulse shaper. In the following, 'resolution' relates to the steepest possible spectral feature which can be experimentally created on shaped pulses, while 'sensitivity' stands for the level of differences between two theoretically assumed shaped spectra which can be discriminated by comparison with the experimental shaped CT. In this context, we regard the atomic system as a spectrally highly sensitive probe (compared to spectrometers used in usual methods) of known response to a shaped light field. First, we observe a strong sensitivity to single-pixel shifts of the shape function. Second, the reproduction of the shaped CT by the numerical solution of the time-dependent Schrödinger equation allows for the retrieval of the actual spectral phase function. In particular, this method could be a tool for testing future very high resolution pulse shapers [14]. Traditional techniques commonly used to characterize pulse shapers such as FROG [15] or SPIDER [16, 17] are well suited to slowly varying spectral phases or amplitudes. Their resolution is, however, limited by the spectrometer used and is, in general, far below the resolution requested to record sharp variations such as phase jumps. It cannot beat the width of an atomic resonance. The particularly interesting feature of our approach is to provide a highly sensitive response not only at resonance, but on the whole spectrum (in practice, half of the spectrum for each sign of the chirp).

The paper is organized as follows: We present the experimental set-up in Sect. 2, the results obtained with a 128 pixels pulse shaper are detailed in Sect. 3. Preliminary results obtained with a high resolution (640 pixels SLM) are finally described in Sect. 4.

✉ Fax: +33-561558317, E-mail: bertrand.girard@irsamc.ups-tlse.fr
*_Present address_: Philipps-Universität Marburg, Institut für Physikalische Chemie, Hans-Meerwein-Strasse, 35032 Marburg, Germany
**_Present address_: CPMOH, 351 cours de la Libération, 33405 Talence Cedex, France

2 Experiment

The laser system (Fig. 1a) comprises a commercial amplified Ti : Sa system (Spitfire Spectra Physics) delivering 795 nm-130 fs-1 mJ pulses as pump and a home-built two-stage non-collinear OPA [18] producing 607 nm-30 fs-3 μJ pulses as probe. The IR light (8 nm-bandwidth) is shaped, negatively chirped with a double-pass grating-pair stretcher, recombined with the visible probe light and sent into a sealed rubidium cell ($T = 85\,^{\circ}\mathrm{C}$ corresponding to a pressure of 4×10^{-5} mbar, for which the propagation effects are negligible [7, 8, 19, 20]). The $5s$–$5p$ ($^2P_{1/2}$) transition is resonantly excited with the shaped chirped pulse (Fig. 1b). The limited spectral width of 8 nm minimizes an excitation to the neighbouring $5p$ ($^2P_{3/2}$) state. Simultaneous excitation would lead to spin wavepackets that induce an additional very fast modulation of the transients. The visible pulse probes the transient excited state population on the ($5p$–ns,$n'd$) transitions. It is much shorter than the dynamics induced by the shaped excitation, which gives us the temporal resolution required. All experiments are performed in the perturbative regime (fluence of 12 μJ/cm^2). The pump-probe signal is detected by monitoring the fluorescence at 420 nm ($6p \rightarrow 5s$) due to the radiative cascade (ns,$n'd$) $\rightarrow 6p \rightarrow 5s$ and collected by a photomultiplier tube as depicted on Fig. 1b.

The shaper realizes an optical Fourier transform with a 1800 g/mm grating and a $f = 14$ cm cylindrical mirror used in off-axis angle that spatially disperses and focuses the optical frequencies on the SLM. Another mirror-grating pair completes the $4-f$-setup that adds in itself zero dispersion to the pulse shape.

The double stack SLM (CRI) with 128 pixels of each 100 μm width allows us to add extra phase shifts to the quadratic phase and to attenuate the spectrum. The phase shift per applied voltage on the SLM has previously been calibrated in the usual way by measuring in a separate setup the rotation of linearly polarized light. The total phase is then

$$\varphi(\omega) = \varphi_{\mathrm{stretcher}}(\omega) + \varphi_{\mathrm{shaper}}(\omega) \qquad (1)$$

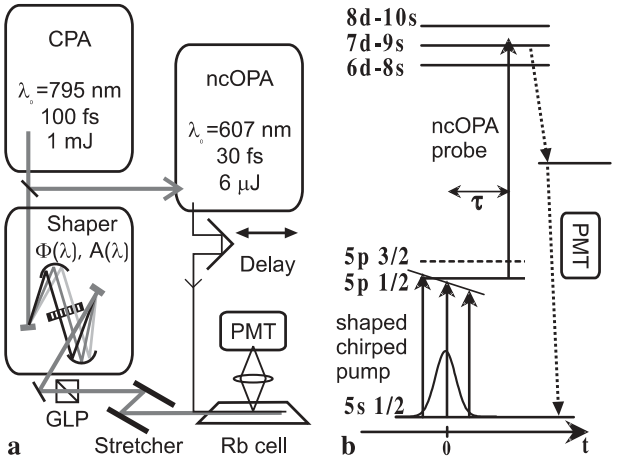

FIGURE 1 **a** Experimental setup. CPA: chirped pulse amplification system, NcOPA: non-collinear optical parametric amplifier, GLP: glan polarizer, PMT: photomultiplier tube. **b** Level schemes and relevant transitions in Rb (the $6p-5s$ fluorescence at 420 nm is recorded by the PMT as a function of pump-probe delay)

$\varphi_{\mathrm{shaper}}(\omega)$ is the shaper phase function and the dispersion induced by the stretcher is mainly quadratic :

$$\varphi_{\mathrm{stretcher}}(\omega) \simeq \frac{1}{2}\varphi''(\omega-\omega_0)^2. \qquad (2)$$

Here $\omega_0 = 2.369$ rad/fs is the resonance angular frequency, φ'' the quadratic dispersion introduced by the stretcher. Higher order terms induce small corrections which do not change qualitatively the main features but are included in the simulations (see below). The CT require a large chirp ($\varphi'' \simeq -9 \times 10^5$ fs^2/rad), corresponding to a pulse duration of about 22 ps. With only the quadratic phase induced by the stretcher (Fig. 2, straight line), we observe an oscillation pattern in the excited state amplitude as shown on Fig. 5a [1]. We refer to this pattern, where the shaper is inactive, as normal CT.

3 Results with a 128 pixels SLM

In a first experiment, the shaper resolution is tested with an amplitude only, time-independent (integral) experiment. Neglecting the aberrations, the expected focal spot [21] of a single frequency Gaussian beam is ca. 1/3 pixel wide. Since the final excited state population of this one-photon excitation is proportional to the intensity at resonance, we use rubidium itself to measure the spread of the resonance frequency on the SLM, i.e., the shaper resolution. To carry on this measurement, we switch off the transmission pixel per pixel and we record the pump-probe signal for a delay much larger than the pulse durations as a function of the off-switched pixel [3]. The result is plotted on Fig. 3. The measured width of the extinction curve is 1.7 pixels FWHM (0.4 nm with dispersion on the SLM of 0.26 nm/pixel). We obtain the same width with a razor blade instead of the SLM and with different beam diameters. Compared to the theoretical limit of ≤ 1 pixel, this value is easily explained by the enlarged spot size in the Fourier plane due to geometrical aberrations from the off-axis $4-f$-setup. Moreover, this value is comparable to the one measured in similar set-ups [22].

This integral measurement characterizes the spot size in the Fourier plane since the resonance frequency is infinitely sharp at our scale. On the other hand, as we will show, time resolved measurements are directly sensitive to the spatial dispersion of the frequencies on the mask. They provide a very high sensitivity over a broad spectral range. The principle is the following: The strong chirp encodes a phase-shaped spectrum onto the temporal CT oscillations, which are then decoded by the time resolving probe pulse [23]. Here, we apply a π-step to the spectral phase at a frequency ω_{step} (Figs. 2 and 4). Then we scan the π-step position away from resonance and observe the transformation of the CT (shown on Fig. 5b–d). Comparing the resulting shapes provides an enhanced sensitivity (exactly as it is possible to measure the center of a spectral line with accuracy much better than its width). It is known that with strongly chirped pulses, the minimum temporal width of an amplitude perturbation is $\sqrt{|\varphi''|}$ [23, 24]. Here, although the perturbation is a step function in the spectral phase, one can show that for a large chirp, this phase step results in a temporal electric field proportional to the unshaped chirped field multiplied by $\mathrm{erf}\left[\sqrt{|\varphi''|}\frac{(1+i)}{2}(\omega_{\mathrm{step}}-\omega_0-\frac{t}{\varphi''})\right]$ [25]. The temporal

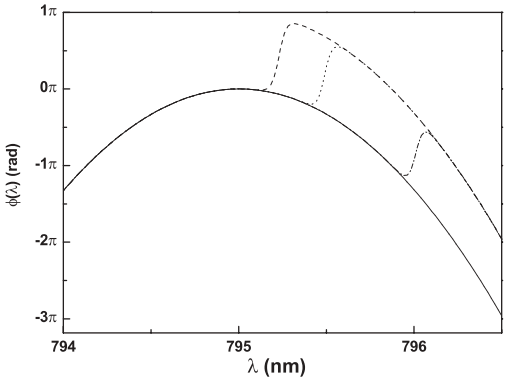

FIGURE 2 Phase functions. Pure quadratic chirp (*straight line*). Shaped phase functions coincide on both ends, but differ on the π step location: 1 pixel below resonance (*dashed*), two pixels below (*dotted*), four pixels below (*dashdotted*); curves take into account the actual resolution

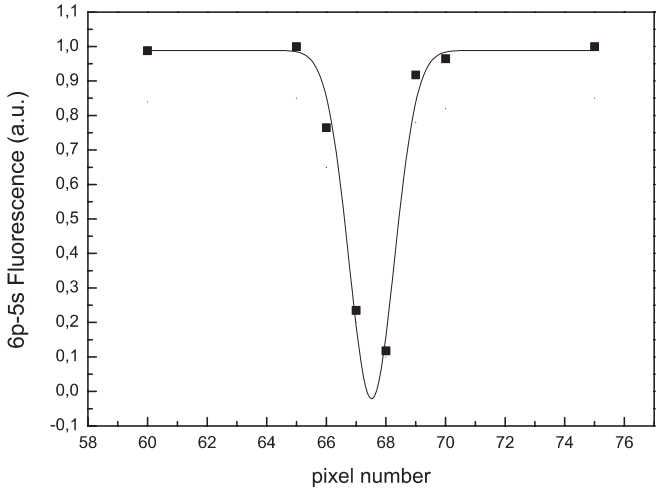

FIGURE 3 Integrated experiment: asymptotic (final) population when one single pixel is extinguished ($H(\omega_n) = 0$) as a function of the pixel number n

half-width (corresponding to a variation of $|\mathrm{erf}(z)|$ from 0 to 0.8) for an ideal sharp spectral step function is $\Delta t \simeq 1.8 \times \sqrt{|\varphi''|} = 1.7$ ps here. The same typical time scale governs the duration of the passage through resonance [1] around ω_0. This minimal width may eventually be enlarged by the smooth spectral step from the limited shaper resolution described in the next paragraph (Fig. 6). Since the CT are a phase diagram of the excitation pulse, we observe on these ones a transition time interval marked as $[t_1, t_2]$ in Fig. 5b–d and defined by $t_{1,2} = (\omega_{\mathrm{step}} - \omega_0)\varphi'' \pm \Delta t$. For $t < t_1$, we have normal CT; For $t > t_2$, the electric field has an inverted sign compared to normal CT and this produces inverted oscillations on the CT.

The shaped CT are modeled using the convolution of the mask function $M(x)$ by the intensity profile of the beam at the mask [10]:

$$H(\omega) \propto \int \mathrm{d}x M(x) \mathrm{e}^{-2(x-\alpha\omega)^2/w_0^2} \tag{3}$$

where α is the spatial dispersion and w_0 the radius of the focused beam at the mask (x is the spatial direction along the mask). This expression is valid if only the fundamental Gaussian mode is dominant which is the case in our experiment where spatial filtering is provided by an iris. Although both diffraction and geometric aberrations contribute to the spot

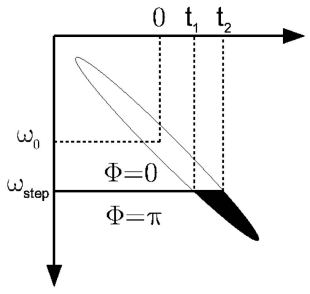

FIGURE 4 Strong chirp of a π-step shaped spectrum. Passage through resonance (ω_0) defines $t = 0$. The steep transition in the frequency domain (of the order of the interpixel gap width) induces a broad transition in the time domain, on an interval $[t_1, t_2]$

shape, as discussed above, we assume that it can be modeled by a Gaussian profile with a width taking all these effects into account. This convolution smoothes the mask function, and it is usually believed that physical features smaller than w_0 on the mask are smeared out. This is effectively true in the case of amplitude only shaping. The situation is different for phase pulse shaping, and more precisely for a π phase step as can be seen in Fig. 6. Effectively, this convolution leads to a hole in the amplitude shape of width ca. w_0/α, and the phase transmission is essentially the expected sharp π-step, except for a short range limited approximately to the gap size. This was already qualitatively explained by Silberberg et al. [2, 26].

In order to achieve the best agreement between theory and experiment, the cubic spectral phase contribution from the stretcher $\varphi_{\mathrm{stretcher}}(\omega) \simeq \frac{1}{2}\varphi''(\omega-\omega_0)^2 + \frac{1}{6}\varphi'''(\omega-\omega_0)^3$ had to be included. The effective values of the chirp φ'', cubic spectral phase φ''' and the time of passage through resonance are adjusted on the normal CT. These parameters are henceforth fixed and used to fit the theoretical shaped CT to the experiment. The adjusted parameters are the step position ω_{step}, and the waist size w_0. The results are displayed in Fig. 5 and an excellent agreement is obtained. The parameters achieving the best fits are given in the figure caption. A very high sensitivity to the step position is observed. The waist size affects mainly the contrast of the first two oscillations, in particular for the step closest to the resonance (Fig. 5d). To check the sensitivity of this scheme to the effective shape of $M(x)$, and in particular to check the steepness of the step, we have also used a step with an adjustable slope in the simulations. No effect is observed for a reasonable value of the waist (ca. 100 μm). As can be expected, the experiment is sensitive to this parameter only for very small values of the waist (less than 25 μm). Indeed, both parameters tend to produce similar effects of smoothing the transition from normal to inverted CT.

Scanning the position of the phase step by a single pixel (or $\delta\omega = 7.75 \times 10^{-4}$ rad/fs) shifts the interval $[t_1, t_2]$ by $\delta t = \varphi''\delta\omega$ (ca. 725 fs here) producing a huge effect as seen in Fig. 5b–d. Thus we retrieve the actual spectral phase functions as shown in Fig. 2 from the measured CT. The effect of varying the step position changes dramatically the balance between the two peaks in the CT closest to the step. This is particularly true for a step close to resonance. Indeed, the hole in the amplitude transmission (Fig. 6a) reduces the available energy at resonance and therefore reduces the asymptotic population transferred. The exact 180° phase of the CT oscil-

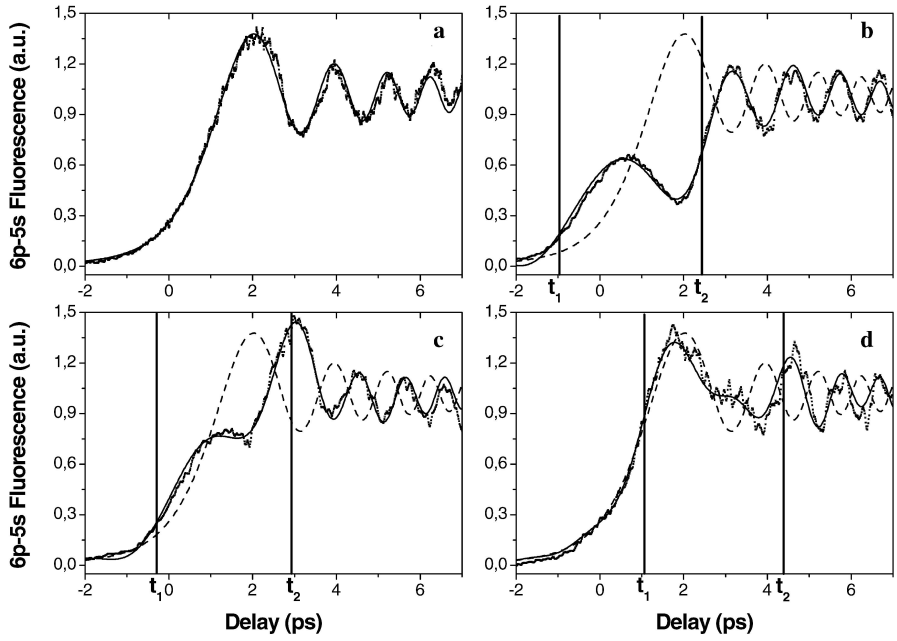

FIGURE 5 Coherent transients in experiment (*dots*) and theory (*lines*) with $\phi'' = -8.9\times10^5$ fs^2, $\phi''' = 1.5\times10^7$ fs^3, $w_0 = 75$ μm. **a** Normal CT. Passage through resonance is at $t = 0$. **b–d** CT with phase π-step, each compared to normal CT (*dashed grey line*): 0.85 pixels below resonance (**b**), 1.85 pixels below resonance (**c**), 4.4 pixels below resonance (**d**); $[t_1, t_2]$: interval of phase transition, of width $|t_2 - t_1| = 2\Delta t \simeq 3.6\times\sqrt{|\phi''|} = 3.4$ ps

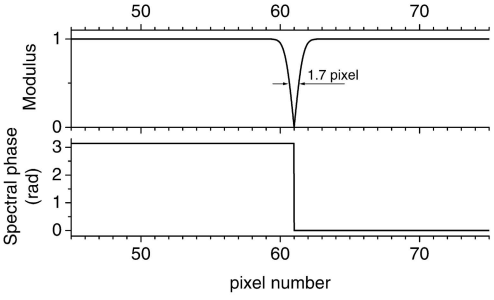

FIGURE 6 Ideal transmission function $H(\omega)$ for an applied π phase step (modulus at the *top*; argument at the *bottom*)

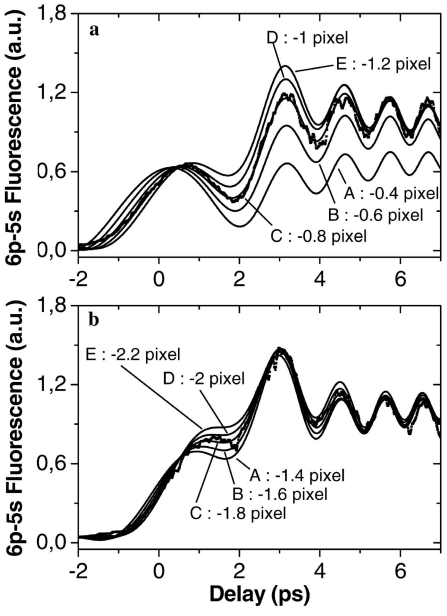

FIGURE 7 Sensitivity of the inverted CT method. Several simulations of inverted CT with π-step positions separated by 1/5 pixel, from $-2/5$ to $+2/5$ pixels away from each experimental π-step. The following parameters are used : $w_0 = 75$ μm, $\phi'' = -8.9\times10^5$ fs^2; $\phi''' = 1.5\times10^7$ fs^3. **a** Experimental step at 0.8 pixel below resonance as in Fig. 5b; **b** Experimental step at 1.8 pixel below resonance as in Fig. 5c

lations for normal and phase-shifted excitation (Fig. 5) shows that the height of the phase step is indeed π and thus confirms the calibration of the SLM. Taking into account that the transition width is $\sqrt{|\varphi''|}$, the ultimate spectral sensitivity concerning the position of the phase step achieved with the CT-retrieval method is mostly limited by the experimental signal to noise ratio. Provided that we are not limited by the probe duration, it could be estimated in our case to about $\sqrt{|\varphi''|}/10 \simeq 100$ fs. As an illustration, Fig. 7 shows simulations with scan steps of 1/5 pixel, corresponding in the time domain to a step of 140 fs. Even in this case, each curve is easily distinguishable and can thus be used to test future pulse shapers where a larger pixel number enables this stronger dispersion on the SLM. With the transition angular frequency $\omega_0 \sim 2.4$ rad/fs, the relative sensitivity $\delta\omega/\omega_0$ is below 10^{-4}. This value depends on the parameters of our study. As can be seen from the argument of the erf function, an increase of the chirp parameter could even improve this sensitivity.

4 Preliminary results with a 640 pixels SLM

In order to illustrate the high sensitivity of the CT method, Fig. 8a shows preliminary results obtained with a 640 pixels dual SLM (Jenoptik). These have been obtained with two independent SLM placed 2 mm apart, allowing for phase and amplitude pulse shaping, although here phase shaping only is used [27]. A long $4-f$ line ($f =$ 600 mm, 2000 gr/mm gratings) provides to this new pulse shaper a resolution of 0.06 nm/pixel. The time window provided by this pulse shaper is ca. 35 ps, allowing one to generate the required chirp (9×10^5 fs^2, slightly above the theoretical Nyquist limit (of 6.5×10^5 fs^2 here) [14]) directly together with the phase step. This provides a pure quadratic phase, without any higher order term. In Fig. 8a, several scans separated by one pixel shift of the π-step are displayed, show-

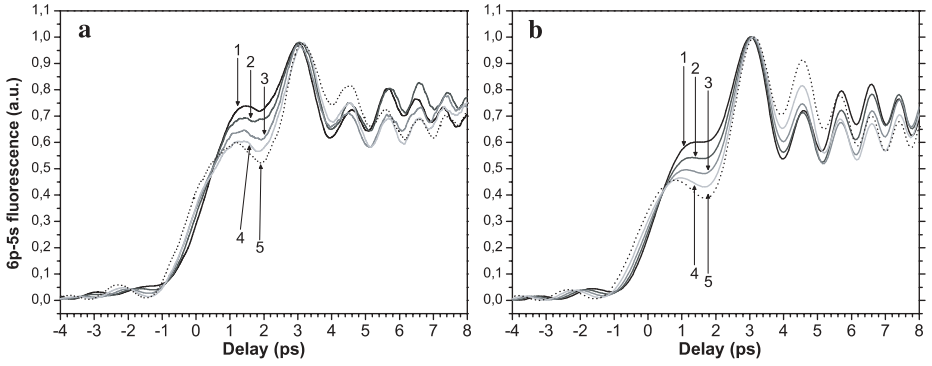

FIGURE 8 Results obtained with a dual 640 pixels pulse shaper. **a** experimental scans with π-phase step shifted by one pixel between each scan, with detunings from resonance ranging from 0.30 nm to 0.54 nm. **b** corresponding simulations

ing again a huge sensitivity. The corresponding simulations are plotted in Fig. 8b, demonstrating an excellent agreement.

5 Conclusion

In this paper, we have shown the extreme sensitivity of the coherent transients to small changes applied to the spectral phase of the pump pulse. Together with a detailed study of the sensitivity of the CT to small spectral shifts of a π phase step, we have presented preliminary results with a 640 pixels SLM inserted in a high resolution $4f$ line. These results stress the advantage of increasing the pulse shaper resolution (which means improving the spectral sampling step) for Coherent Transients experiments in simple systems.

To apply the CT shaper testing method, an atomic resonance lying within the pulse spectrum is required. Up or down chirp is chosen such that the resonance is crossed early, leading to long oscillations [1]. The population scales down linearly, but the CT oscillation inversion point could be demonstrated over the entire spectrum while maintaining the same signal to noise ratio. Then, the atomic transition sharpness makes single pixel phase modulation shifts visible.

The CT method provides a simple, yet rich test system for high resolution femtosecond pulse shaping, such as needed for new shapers [14]. Moreover since atomic transitions can be found in a very broad spectral range, this method provides a tool to observe shaping effects in spectral domains where usual methods cannot be used.

Finally, the fidelity of the experiment to the integration of the time-dependent Schrödinger equation has been demonstrated. This opens the route to the open-loop application of theoretical pulse shapes to more complex control schemes.

ACKNOWLEDGEMENTS We sincerely acknowledge F. Rosca-Pruna for her help at the final stage of the experiment and C. Dorrer for fruitful discussions. We thank Prof. K.L. Kompa for his generous support of this study. We also acknowledge financial support from the European Union (contract HPRN-CT-1999-00129, COCOMO), the ESF ULTRA program, Univ. P. Sabatier "Actions Ponctuelles de Coopération" program, Contrat de plan-Etat Région 2000-6 "Spectroscopies Optiques Ultimes".

REFERENCES

1 S. Zamith, J. Degert, S. Stock, B. de Beauvoir, V. Blanchet, M.A. Bouchene, B. Girard: Phys. Rev. Lett. **87**, 033 001 (2001)
2 N. Dudovich, D. Oron, Y. Silberberg: Phys. Rev. Lett. **88**, 123004 (2002)
3 J. Degert, W. Wohlleben, B. Chatel, M. Motzkus, B. Girard: Phys. Rev. Lett. **89**, 203 003 (2002)
4 J.B. Ballard, H.U. Stauffer, E. Mirowski, S.R. Leone: Phys. Rev. A **66**, 043 402 (2002)
5 R. Netz, T. Feurer, G. Roberts, R. Sauerbrey: Phys. Rev. A **65**, 043 406 (2002)
6 R. Netz, A. Nazarkin, R. Sauerbrey: Phys. Rev. Lett. **90**, 063 001 (2003)
7 J.E. Rothenberg: IEEE J. Quantum Electron. **QE-22**, 174 (1986)
8 J.T. Manassah: Appl. Opt. **25**, 3980 (1986)
9 M.M. Wefers, K.A. Nelson: J. Opt. Soc. Am. B **12**, 1343 (1995)
10 A.M. Weiner: Rev. Sci. Instr. **71**, 1929 (2000)
11 M.A. Dugan, J.X. Tull, W.S. Warren: J. Opt. Soc. Am. B **14**, 2348 (1997)
12 E. Zeek, K. Maginnis, S. Backus, U. Russek, M.M. Murnane, G. Mourou, H.C. Kapteyn: Opt. Lett. **24**, 493 (1999)
13 F. Verluise, V. Laude, Z. Cheng, C. Spielmann, P. Tournois: Opt. Lett. **25**, 575 (2000)
14 G. Stobrawa, M. Hacker, T. Feurer, D. Zeidler, M. Motzkus, F. Reichel: Appl. Phys. B **72**, 627 (2001)
15 K.W. DeLong, R. Trebino: J. Opt. Soc. Am. A **10**, 1101 (1993)
16 C. Iaconis, I.A. Walmsley: Opt. Lett. **23**, 792 (1998)
17 C. Dorrer, B. de Beauvoir, C. Le Blanc, J.P. Rousseau, R. Ranc, P. Rousseau, J.P. Chambaret, F. Salin: Appl. Phys. B **70**, S77 (2000)
18 E. Riedle, M. Beutter, S. Lochbrunner, J. Piel, S. Schenkl, S. Spörlein, W. Zinth: Appl. Phys. B **71**, 457 (2000)
19 J.C. Delagnes, V. Blanchet, M.A. Bouchene: Opt. Commun. **227**, 125 (2003)
20 M. Jacquey, S. Bonhommeau, M.A. Bouchene: Opt. Lett. **28**, 1272 (2003)
21 M.M. Wefers, K.A. Nelson: IEEE J. Quantum Electron. **QE-32**, 161 (1996)
22 J.B. Ballard, H.U. Stauffer, Z. Amitay, S.R. Leone: J. Chem. Phys. **116**, 1350 (2002)
23 F.G. Sun, Z. Jiang, X.C. Zhang: Appl. Phys. Lett. **73**, 2233 (1998)
24 J.P. Geindre, P. Audebert, S. Rebibo, J.-C. Gauthier: Opt. Lett. **26**, 1612 (2001)
25 J. Degert: in *Thesis* (Univ. P. Sabatier, Toulouse 2002)
26 D. Meshulach, Y. Silberberg: Phys. Rev. A **60**, 1287 (1999)
27 A. Monmayrant, B. Chatel: Rev. Sci. Instrum. in press (2004)